Susceptibility of pediatric acute lymphoblastic leukemia to STAT3 inhibition depends on p53 induction

Luca Gasparoli,[1] Clemence Virely,[1] Alexia Tsakaneli,[1] Noelia Che,[1] Darren Edwards,[2] Jack Bartram,[2] Michael Hubank,[3] Deepali Pal,[4] Olaf Heidenreich,[5] Joost H.A. Martens,[6] Jasper de Boer[1] and Owen Williams[1]

[1]Cancer Section, Developmental Biology and Cancer Department, UCL Great Ormond Street Institute of Child Health, London, UK; [2]Department of Pediatric Hematology, Great Ormond Street Hospital for Children, London, UK; [3]Center for Molecular Pathology, The Royal Marsden, Sutton, UK; [4]Department of Applied Sciences, Northumbria University, Newcastle upon Tyne, UK; [5]Princess Maxima Center for Pediatric Oncology, Utrecht, the Netherlands and [6]Department of Molecular Biology, Faculty of Science, Radboud Institute for Molecular Life Sciences, Radboud University, Nijmegen, the Netherlands

Correspondence: O. Williams
owen.williams@ucl.ac.uk

Received: May 25, 2023.
Accepted: September 27, 2023.
Early view: October 5, 2023.

https://doi.org/10.3324/haematol.2023.283613

Abstract

Advances in the clinical management of pediatric B-cell acute lymphoblastic leukemia (B-ALL) have dramatically improved outcomes for this disease. However, relapsed and high-risk disease still contribute to significant numbers of treatment failures. Development of new, broad range therapies is urgently needed for these cases. We previously reported the susceptibility of *ETV6-RUNX1*$^+$ pediatric B-ALL to inhibition of signal transducer and activator of transcription 3 (STAT3) activity. In the present study, we demonstrate that pharmacological or genetic inhibition of STAT3 results in p53 induction and that CRISPR-mediated *TP53* knockout substantially reverses susceptibility to STAT3 inhibition. Furthermore, we demonstrate that sensitivity to STAT3 inhibition in patient-derived xenograft (PDX) B-ALL samples is not restricted to any particular disease subtype, but rather depends on *TP53* status, the only resistant samples being *TP53* mutant. Induction of p53 following STAT3 inhibition is not directly dependent on MDM2 but correlates with degradation of MDM4. As such, STAT3 inhibition exhibits synergistic *in vitro* and *in vivo* anti-leukemia activity when combined with MDM2 inhibition. Taken together with the relatively low frequency of *TP53* mutations in this disease, these data support the future development of combined STAT3/MDM2 inhibition in the therapy of refractory and relapsed pediatric B-ALL.

Introduction

Pediatric leukemia accounts for up to a fifth of all cancer deaths in children. Acute lymphoblastic leukemia (ALL) comprises half of these cases, despite the success of modern chemotherapy and risk stratification. Failure of therapy in pediatric ALL is due to refractory and relapsed disease, as well as the toxicity of the chemotherapy itself.[1] There is, therefore, an unmet clinical need that may be addressed by focusing on inhibition of oncogenic pathways required for leukemia maintenance across a broad range of disease subtypes. Targeting susceptibilities retained in relapsed leukemia is particularly relevant in this context.

Cancer cells often exhibit an exaggerated dependence upon normal cellular signaling pathways. Identification of such pathways deregulated in B-cell precursor ALL (B-ALL) and essential for leukemia survival is crucial for the development of novel therapies. For example, aberrant activation of STAT3 has been linked with transformation and tumor growth in multiple tissues.[2] Indeed, the importance of STAT3 in hematopoietic malignancies is well documented, particularly for subtypes of lymphoma[3] and acute myeloid leukemia.[4] Although STAT3 is required for the normal reconstitution activity of hematopoietic stem cells[5,6] its pharmacological targeting does not appear to elicit short-term toxicity,[7] providing a rationale for development of STAT3-targeting drugs.[8] STAT3 is also required for normal B-cell development, deficiency resulting in reduced numbers of early B-cell progenitors.[9] STAT3-deficient pro-B cells exhibit elevated levels of apoptosis, suggesting that impaired B-cell development is caused by loss of B-cell progenitor viability in the absence of STAT3.[9]

We previously demonstrated that STAT3 signaling plays an essential role in the most common form of pediatric leukemia, t(12;21) B-ALL. Thus, B-ALL cell lines containing the t(12;21) chromosomal translocation, which encodes the ETV6-RUNX1 fusion protein, are highly dependent on STAT3 signaling for leukemia growth, survival, clonogenicity and progression *in vivo*.[10] Furthermore, patient primary *ETV6-RUNX1*$^+$ B-ALL cells

were also found to be sensitive to STAT3 inhibition. Activation of STAT3 was mediated by an intracellular mechanism downstream of the ETV6-RUNX1 fusion protein, involving guanine nucleotide exchange factor induction.[11] Other B-ALL subtypes, with a much poorer prognosis, were also found to be dependent upon sustained STAT3 activity.[10] More recently, STAT3 dependence has also been demonstrated in poor-risk pediatric B-ALL subtypes, with high STAT3 expression being associated with inferior survival.[12] Although it is likely that there are distinct mechanisms responsible for STAT3 activation in the different B-ALL subtypes, dependency renders them susceptible to pharmacological inhibition of STAT3.

In this study, we used global gene expression analysis to demonstrate that STAT3 inhibition leads to induction of the p53 response in B-ALL cells. Pharmacological inhibition, small hairpin RNA (shRNA)-mediated knockdown and CRISPR/Cas9-mediated ablation of STAT3 all result in elevated p53 protein and p53-target gene expression. B-ALL apoptosis in response to STAT3 inhibition can be reversed by deletion of *TP53*. In contrast to the subtype-specific STAT3 dependence we observed previously in B-ALL cell lines,[10] patient-derived xenograft (PDX) B-ALL samples exhibited broad susceptibility to STAT3 inhibition across different subtypes, with resistance only apparent in two *TP53* mutant samples. These data suggest that requirement for STAT3 activity may be a general characteristic of the pediatric B-ALL lineage, perhaps associated with signaling pathways operating in the cells of origin. Enhanced elimination of B-ALL cells was achieved by combining STAT3 inhibition with p53 induction through inhibition of MDM2, indicating a novel potential therapeutic opportunity. Indeed, since only a minority of pediatric B-ALL cases are associated with *TP53* mutations,[13] even in high-risk and relapsed disease,[14-16] induction of p53 may be an attractive therapeutic approach to leukemias that are refractive to conventional therapy.

Methods

Mice

Mice were maintained in UCL GOSICH animal facilities and experiments were performed according to and approved by United Kingdom Home Office regulations and followed UCL GOSICH institutional guidelines.

B-cell acute lymphoblastic leukemia patient-derived xenograft acute lymphoblastic leukemia cells

Ethical approval was given (Research Ethics Committee reference 14/EM/0134) for use of appropriately consented material from patients with B-ALL at Great Ormond Street Hospital for Children (London, UK). Non-irradiated 6- to 12-week-old NOD-SCID-$\gamma^{-/-}$ (NSG; The Jackson Laboratory, Bar Harbor, ME, USA) mice were intra-bone injected with 1-2x10^6 mononuclear cells (*Online Supplementary Table S1*). Recipient mice were sacrificed upon developing clinical signs of disease. Human PDX ALL cells were harvested and purified from spleens using the mouse cell depletion kit (Miltenyi Biotec, Surrey, UK).

Cell culture and reagents

For co-culture experiments with Luciferase-expressing B-ALL PDX samples, 3x10^4/cm^2 mesenchymal stem cells (MSC) were plated in 96-well tissue culture plates and 2x10^4 B-ALL PDX cells were added in StemSpan Serum-Free Expansion Medium II (SFEM II, STEMCELL Technologies, Cambridge, UK).[17,18] Cells were treated for 5 days with indicated drugs and luminescence analyzed with the Steady-Glo Luciferase Assay System (Promega, Southampton, UK), according to manufacturer's instruction, and detected with Infinite m200 Pro microplate reader (Tecan, Reading, UK). The following reagents and inhibitors were used, S3I-201 (Cayman Chemical, MI, USA), Napabucasin (BBI608; MedChemExpress, NJ, USA), C188-9 (MedChemExpress and Adooq Biosciences, CA, USA), Nutlin-3a (Merck Life Science, Dorset, UK) and Idasanutlin (Bio-Techne, Abingdon, UK).

In vivo transplantation

Non-irradiated NSG mice were intravenously transplanted with 2x10^5 luciferase-expressing B-ALL PDX cells. Recipient mice were imaged using the IVIS® Lumina Series III (Perkin-Elmer, Beaconsfield, UK) and randomly allocated to control or drug-treated groups, by flipping a coin. Recipient mice were treated with vehicle (7% dimtehyl sulfoxide [DMSO], 56% Labrasol, 37% polyethylene glycol 400), C188-9 (100 mg/kg), Idasanutlin (30 mg/kg) or C188-9 + Idasanutlin by 5-7 daily oral gavages. No blinding was used.

Quantitative real-time polymerase chain reaction analysis

Quantitative real-time polymerase chain recation (qRT-PCR) was performed on mRNA using TaqMan probe-based chemistry, as previously described,[19] using a StepOnePlus Real-Time PCR System (Thermo Fisher Scientific). Primer/probe sets were from Applied Biosystems, Life Technologies.

Western blot and immunoprecipitation analysis

Western blot and immunoprecipitation (IP) analyses were performed as previously described[10,20] (detailed in the *Online Supplementary Appendix*).

RNA sequencing and chromatin immunoprecipitation sequencing

RNA sequencing (RNA-seq), chromatin immunoprecipitation sequencing (ChIP-seq), ChIP-qPCR and gene set enrichment analysis (GSEA) was performed as detailed in the *Online Supplementary Appendix*.

Statistics

Statistical significance was determined using Prism (GraphPad) software. Statistical analysis of means was performed using the one sample *t* test or unpaired Student's *t* test, two-tailed *P* values <0.05 being considered statistically significant.

Variance was similar between groups. Statistical analysis of survival curves was performed using the log-rank test.

Data availability

The data generated in this study are available within the article and its *Online Supplementary Appendix*. The RNA-seq data generated in this study are publicly available in the Gene Expression Omnibus at GSE179333 (S3I-201) and GSE179332 (shSTAT3) and the ChIP-seq data at GSE213766. More details are provided in the *Online Supplementary Appendix*.

Results

In order to further investigate the mechanism responsible for STAT3 dependency in *ETV6-RUNX1*$^{+}$ B-ALL, we performed RNA-seq in REH cells to examine global gene expression changes 6 hours after pharmacological inhibition of STAT3, via the STAT3 inhibitor S3I-201[21] (Figure 1A). Inhibition of STAT3 resulted in a total of 1,085 significantly upregulated and 820 downregulated genes, of which 156 and 22 were changed more than 2-fold, respectively. We performed GSEA with the MSigDB hallmark gene set collection to identify cellular pathways perturbed in this RNA-seq data in an unbiased manner. The hallmark p53 pathway (M5939) gene set was the most upregulated gene set in this analysis (*Online Supplementary Figure S1A*). Enrichment of high-confidence p53 target genes, assembled in a recent meta-analysis,[22] confirmed that gene expression changes resulting from acute STAT3 inhibition are consistent with p53 induction (Figure 1B). Analysis of *TP53* RNA sequences from the RNA-seq data confirmed that the REH cells were *TP53* wild-type. Next, we performed RNA-seq in REH cells after shRNA-mediated *STAT3* silencing (Figure 1A; *Online Supplementary Figure S1B*). The hallmark p53 pathway was once more the most upregulated gene set (*Online Supplementary Figure S1A*) and high-confidence p53 target genes were significantly enriched in these gene expression changes (Figure 1B). Furthermore, 240 of the 1,085 genes induced by S3I-201 were also significantly upregulated following *STAT3* silencing, 45 of which were high-confidence p53 target genes.[22] Taken together, these data suggest that STAT3 functions in these cells to repress p53 induction. Direct repression of *TP53* by STAT3 has so far only been demonstrated in transformed fibroblast cells, where STAT3 binds to the promoter of *TP53* and inhibits its transcription.[23] However, we did not observe a significant change in *TP53* expression in either of the RNA-seq data sets (fold change [FC] =1.01, *P adj* =0.96 and FC=0.99, *P adj*=0.83 for *TP53* in the S3I-201 and shSTAT3 data sets, respectively). This indicates that p53 induction resulting from STAT3 inhibition was not due to transcriptional activation of *TP53*.

In order to examine whether p53 induction following inhibition of STAT3 occurred at the protein level, we examined p53 protein expression after pharmacological or genetic inhibition of STAT3 (Figure 1C-E). Total p53 protein levels increased significantly in REH cells after 6-hour exposure to S3I-201 and an independent STAT3 inhibitor, Napabucasin (BBI608) (Figure 1C).[24] Moreover, this resulted in increased expression of *CDKN1A* (Figure 1F) and other selected p53 target genes (*Online Supplementary Figure S1C*). shRNA-mediated silencing of *STAT3* (*Online Supplementary Figure S1B*) also resulted in increased total p53 protein and target gene expression (Figure 1D, G). In order to confirm these data using an independent approach, we then targeted *STAT3* in REH cells by CRISPR/Cas9 knockout using two independent gRNA against the regions encoding the SH2 (g1_STAT3) and DNA-binding (g2_STAT3) domains. Tracking of insertions and deletions (Indel) by DEcomposition (TIDE) analysis in the bulk population of STAT3$^{-/-}$ REH cells confirmed the specific and efficient editing of the targeted regions in STAT3 (*Online Supplementary Figure S2A*) and consequent reduction of total STAT3 protein expression in REH cells (Figure 1E). Loss of STAT3 expression led to selective depletion of STAT3$^{-/-}$ REH cells (*Online Supplementary Figure S2B, C*), in line with the anti-proliferative and apoptotic consequences of STAT3 inhibition we described previously.[10] Knockout of STAT3 also resulted in a significant increase in p53 protein (Figure 1E) and target gene (Figure 1H; *Online Supplementary Figure S2D*) expression. Conversely, expression of a constitutively active form of STAT3 (CASTAT3) (*Online Supplementary Figure S3A*) we observed a small but significant decrease in p53 target gene expression (*Online Supplementary Figure S3B*).

Protein levels of p53 are tightly regulated by the E3 ubiquitin ligase MDM2, which targets p53 for ubiquitination and subsequent degradation.[25-27] In order to evaluate the role of MDM2 in controlling p53 protein levels in the context of STAT3 inhibition, we performed immunoprecipitation experiments with a specific MDM2 antibody following a short 6-hour exposure to S3I-201. We observed no changes in MDM2 association with p53 (*Online Supplementary Figure S4A*), an interaction important for MDM2 regulation of p53 protein expression levels.[28] Furthermore, 6 hours after exposure, no changes in total MDM2 protein expression were detected following STAT3 inhibition with either S3I-201 or Napabucasin (*Online Supplementary Figure S4B*). In contrast, MDM2 gene expression increased significantly following STAT3 inhibition (*Online Supplementary Figure S4C*), most likely as a consequence of p53 induction, since MDM2 is a well-described p53 target.[29,30] In summary, no changes in MDM2:p53 interaction or total MDM2 protein expression could be detected at a time point in which p53 induction was evident. Taken together, these data indicate that p53 induction following STAT3 inhibition is not directly dependent on MDM2. Ubiquitination of p53 by MDM2 has also been shown to be positively regulated by MDM4,[31] suggesting an alternative mechanism through which STAT3 could influence p53 protein levels. Although the association of p53 with MDM4 was not affected by 6-hour exposure to S3I-201 (Figure 2A), S3I-201 treatment (Figure 2B) or shRNA-mediated *STAT3* silencing (Figure 2C) resulted in decreased total MDM4 protein expression. Moreover, S3I-201

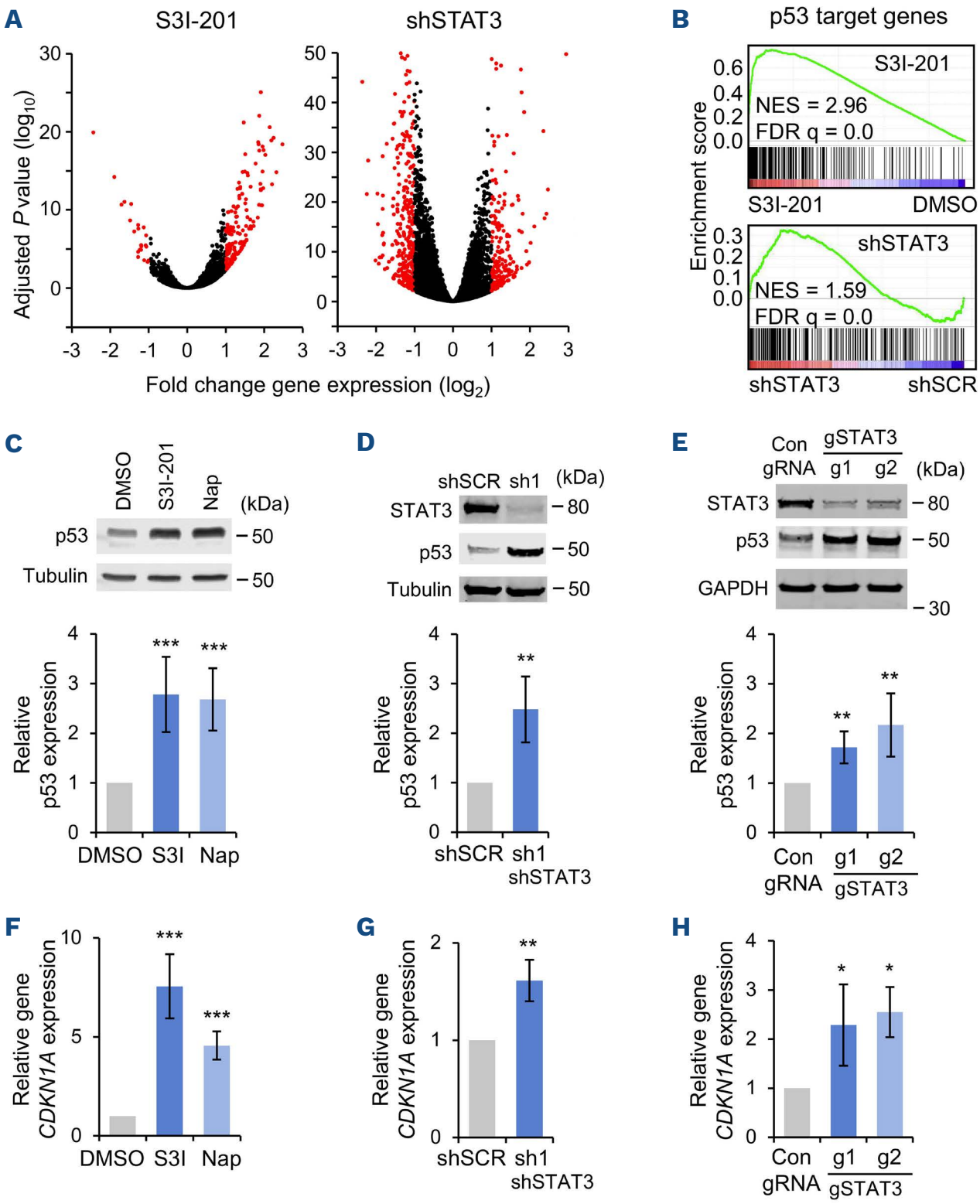

Figure 1. STAT3 inhibition results in p53 induction in B-cell acute lymphoblastic leukemia cells. (A) Volcano plots of RNA-sequencing (RNA-seq) analysis showing fold gene expression changes in REH cells following treatment with S3I-201 (50 μM, 6 hours [hrs], N=3) or 5 days after small hairpin RNA (shRNA)-mediated *STAT3* (sh1, N=3) silencing. Expression changes greater than 2-fold and *P*<0.05 are shown in red, Wald test. (B) Gene set enrichment analysis (GSEA) demonstrating enrichment of p53 target genes, as previously defined in,[22] in S3I-201 and shSTAT3 induced gene expression changes. (C-E) Western blot examples (top panels) and quantification (lower panels) of p53 protein expression in REH cells (C) 6 hours after exposure to S3I-201 (50 μM) or Napabucasin (10 μM), (D) 5 days after transduction with scrambled control or shSTAT3 (sh1) shRNA or (E) 7 days after transduction with Cas9 and control or gSTAT3 gRNA. Bars and error bars are means and standard deviation (SD) of (C) N=8 and (D), (E) N=4 independent experiments. Data are normalized to (C, D) tubulin and (E) GAPDH loading control and to (C) dimethyl sulfoxide (DMSO)-treated, (D) control shRNA transduced and (E) control gRNA transduced REH cells. **P*< 0.05; ***P*<0.01; ****P*<0.001, one sample *t* test. (F-H) quantitative real-time polymerase chain reaction analysis of *CDKN1A* gene expression in REH cells (F) 6 hrs after exposure to S3I-201 (50 μM) or Napabucasin (10 μM), (G) 5 days after transduction with scrambled control or shSTAT3 shRNA or (H) 7 days after transduction with Cas9 and control or gSTAT3 gRNA. Bars and error bars are means and SD of (F) N=5, (G) N=4 and (H) N=5 independent experiments. Gene expression data are normalized to (F) DMSO-treated, (G) control shRNA transduced and (H) control gRNA transduced REH cells. **P*<0.05; ***P*<0.01; ****P*<0.001, one sample *t* test.

induced MDM4 loss was rescued by proteasomal inhibition (Figure 2D) suggesting that it was caused by proteasomal degradation. These data indicate that p53 induction correlates with reduced levels of MDM4 protein expression following STAT3 inhibition.

We speculated that the observed increase in p53 protein expression would translate into increased binding to target gene loci. Indeed, immunoprecipitation experiments following

STAT3 inhibition by S3I-201 revealed a significant increase in the mono-methylation of lysine 372 of p53 (Figure 3A), a post-translational modification of p53 associated with increased DNA binding, resulting from the increase in total p53.[32] Increased binding of target loci by p53 was confirmed by ChIP-seq (Figure 3B, C; *Online Supplementary Figure S4D*) and ChIP-qPCR (Figure 3D) experiments. S3I-201 exposure resulted in more than 2-fold increased binding of p53 at 400 peaks in REH cells (Figure 3B), including well-established p53 target genes *CDKN1A*,[33] *BBC3* (PUMA)[34] and ATF3[35] (Figure 3C, D). GSEA revealed significant enrichment of the genes that were associated with increased p53 binding in gene expression changes following S3I-201 treatment of REH cells (Figure 3E).

In order to determine the contribution of p53 induction to the response of REH cells to STAT3 inhibition, we performed CRISPR/Cas9-mediated knockout of *TP53* in REH cells. Loss of p53 protein was confirmed in two independent *TP53*$^{-/-}$ clones (Figure 4A). TIDE analysis of the *TP53*$^{-/-}$ clones confirmed specific and efficient editing of the targeted region encoding the N-terminus domain of p53 (*Online Supplementary Figure S5A*). As expected, loss of *TP53* abrogated the induction of p53 target gene expression resulting from STAT3 inhibition (Figure 4B) and significantly attenuated apoptosis induction following STAT3 inhibition with either S3I-201 or Napabucasin (Figure 4C). Similar impairment of apoptosis induction was observed following treatment of *TP53*$^{-/-}$ REH clones with the

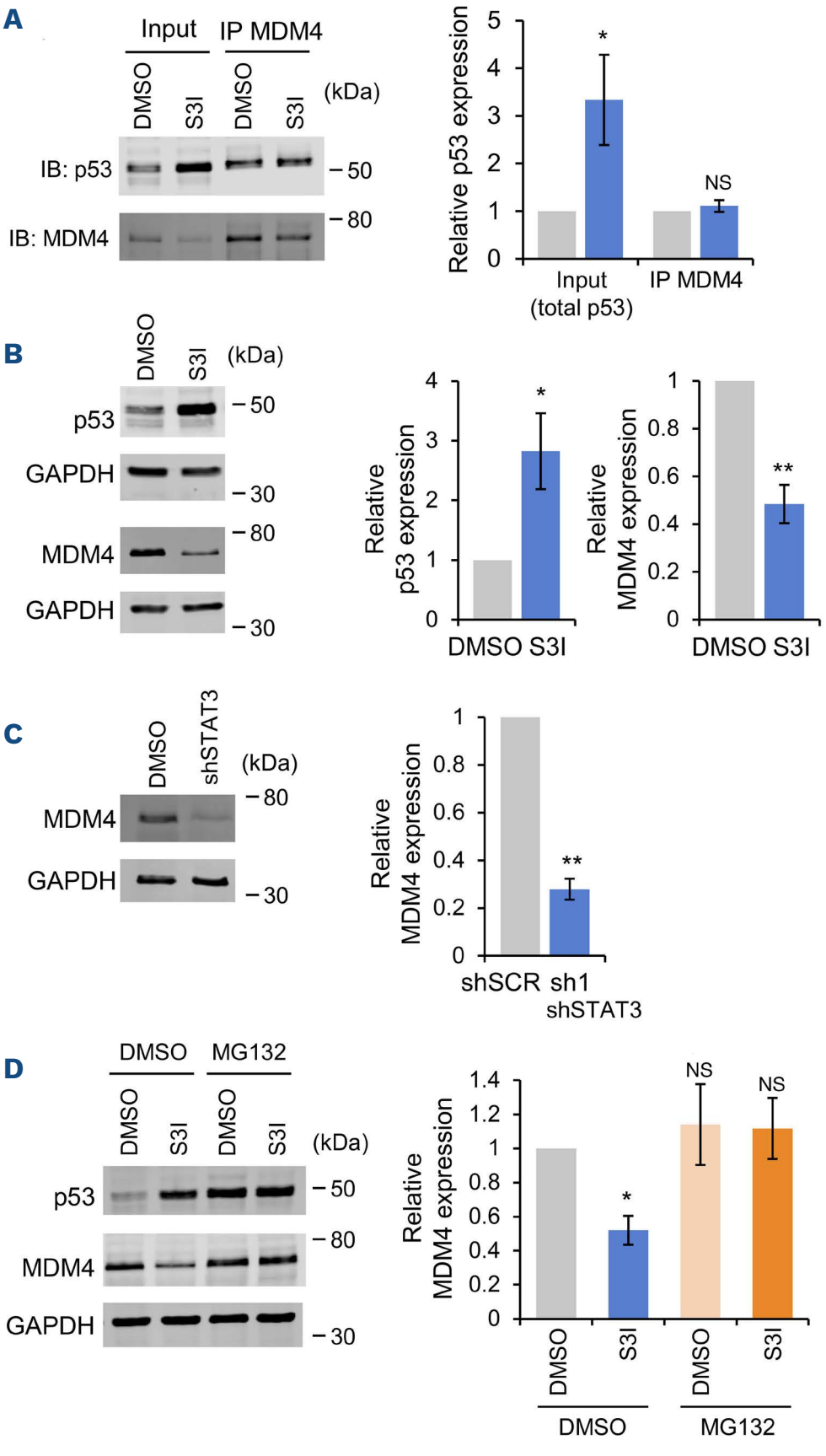

Figure 2. p53 induction following STAT3 inhibition correlates with loss of MDM4. (A) Western blot analysis (left panel) and p53 protein expression quantification (right panel) of input and anti-MDM4 immunoprecipitates from REH cells, following 6-hour treatment with S3I-201 (50 μM). Blots were stained with anti-p53 or anti-MDM4. Data are normalized to dimethyl sulfoxide (DMSO)-treated REH cells. Bars and error bars are means and standard deviation (SD) of N=3 independent experiments. *P<0.05; NS: not significant, one sample *t* test. (B, C) Western blot analysis (left panels) and quantification (right panels) of MDM4 and p53 protein expression in REH cells following (B) 6-hour treatment with S3I-201 (50 μM) or (C) 5 days after transduction with scrambled control or small hairpin STA3 (shSTAT3) (sh1) shRNA. GAPDH was used as a loading control. Bars and error bars are means and SD of N=3 independent experiments. Data are normalized to GAPDH loading control and to DMSO-treated REH cells. *P<0.05; **P<0.01; NS: not significant, one sample *t* test. (D) Western blot analysis (left panel) and quantification (right panel) of MDM4 protein expression in REH cells following 6-hour treatment with S3I-201 (50 μM), with and without MG132 (10 μM). GAPDH was used as a loading control. Bars and error bars are means and SD of N=3 independent experiments. Data are normalized to GAPDH loading control and to DMSO-treated REH cells. *P<0.05; NS: not significant, one sample *t* test.

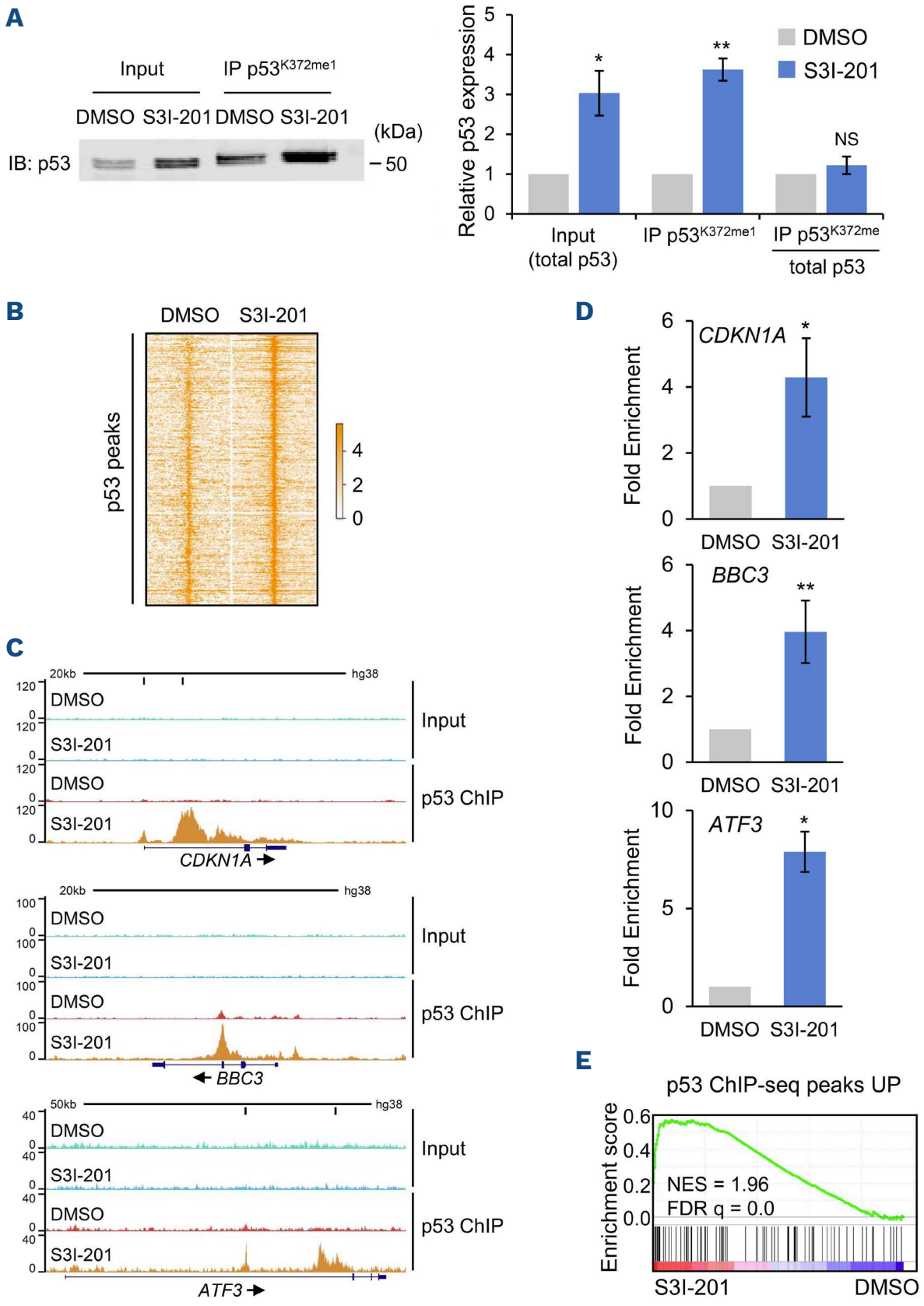

Figure 3. STAT3 inhibition results in increased binding of p53 to target genes. (A) Western blot example (left panel) and quantification (right panel) of input and anti-p53^{K372me1} immunoprecipitates from REH cells, following 6-hour treatment with dimethyl sulfoxide (DMSO) or S3I-201 (50 μM), stained with anti-p53 (DO-1). Bar and error bars are means and standard deviation (SD) of N=3 independent experiments. Data are normalized to DMSO-treated cells. ***P*<0.01, one sample *t* test. (B) Heatmap showing chromatin immunoprecipitation (ChIP) signal for the dynamic p53 peaks (>2-fold increased in S3I-201 with over 100 counts per million reads) following 6-hour exposure to DMSO or S3I-201 (50 μM). (C) Exemplar ChIP-sequencing tracks for p53 peaks at target genes in DMSO- and S3I-201-treated REH cells. High-confidence (*CDKN1A, ATF3*) p53 binding motifs are indicated by vertical black bars below the scale ruler. (D) ChIP quantitative polymerase chain reaction (ChIP-qPCR) validation analysis of p53 binding at *CDKN1A* (top panel), *BBC3* (middle panel) and *ATF3* (lower panel) in REH cells following 6-hour treatment with S3I-201 (50 μM). Data are shown as fold increase of enrichment over that from a gene desert region, normalized to DMSO-treated cells. Bars and error bars are means and SD of N=3 independent experiments. **P*< 0.05; ***P*<0.01, one sample *t* test. (E) Gene set enrichment analysis (GSEA) demonstrating enrichment of 122 genes, with >2-fold increased p53 binding with peaks over 100 cpm reads, in gene expression changes in REH cells following treatment with S3I-201 (Figure 1A).

MDM2 inhibitor Nutlin-3a (Figure 4D). Moreover, *TP53* loss also rescued inhibition of REH cell colony formation in methylcellulose following STAT3 inhibition (*Online Supplementary Figure S5B*). In contrast, S3I-201-induced loss of MDM4 protein was not affected by TP53 knockout, confirming that although p53 has been shown to repress *MDM4* mRNA translation[31] this

was not the cause of MDM4 loss following STAT3 inhibition (*Online Supplementary Figure S5C*).

We demonstrated previously that *ETV6-RUNX1*$^{+}$ B-ALL cell lines and primary patient samples are highly dependent on STAT3 signaling for leukemia growth, survival, clonogenicity and progression *in vivo*.[10] In order to investigate STAT3 dependence

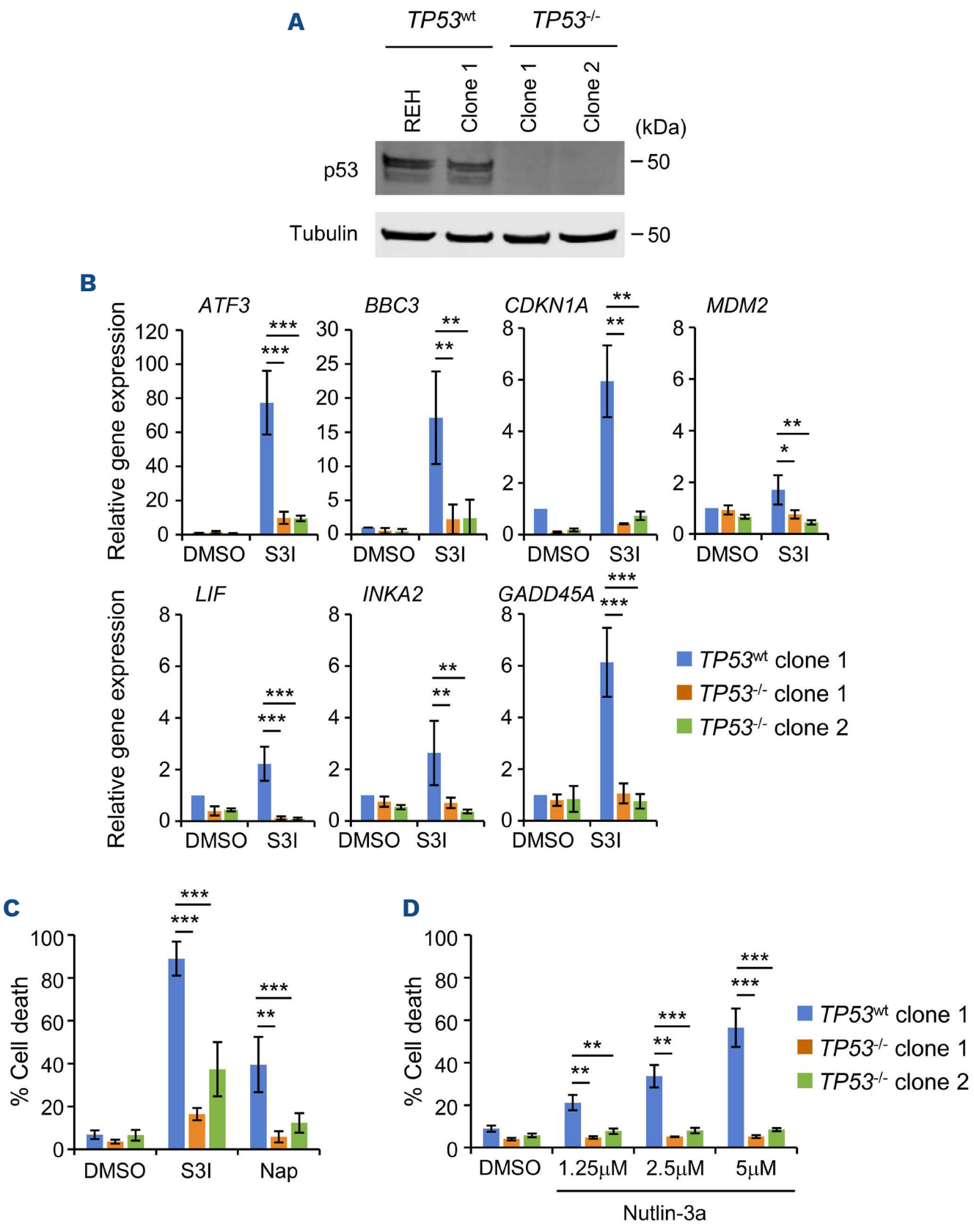

Figure 4. *TP53* knockout desensitizes B-cell acute lymphoblastic leukemia cells to STAT3 inhibition. (A) Western blot analysis of p53 protein expression in REH cells and *TP53*^{wt} and *TP53*$^{-/-}$ clones, obtained by transduction of REH cells with Cas9 and control or *TP53*-specific gRNA, clones from the latter being selected for loss of p53 protein expression. (B) Quantitative real-time polymerase chain reaction (qRT-PCR) analysis of selected p53 target gene[22] expression in *TP53*^{wt} and *TP53*$^{-/-}$ REH clones following 6-hour treatment with S3I-201 (50 μM). Gene expression data are normalized to gene expression in the dimethyl sulfoxide (DMSO)-treated *TP53*^{wt} clone. Bars and error bars are means and standard deviation (SD) of N=4 independent experiments. *P<0.05; **P<0.01; ***P<0.001, unpaired Student's *t* test between S3I-201-treated *TP53*^{wt} and *TP53*$^{-/-}$ clones. (C) Induction of apoptosis (% Annexin V^{+} cells) in *TP53*^{wt} and *TP53*$^{-/-}$ REH clones following 48 hours treatment with S3I-201 (50 μM) or Napabucasin (10 μM). Bars and error bars are means and SD of N=5 independent experiments. **P<0.01; ***P<0.001, unpaired Student's *t* test between S3I-201- or Napabucasin-treated *TP53*^{wt} and *TP53*$^{-/-}$ clones. (D) Induction of apoptosis (% Annexin V^{+} cells) in *TP53*^{wt} and *TP53*$^{-/-}$ REH clones following 48-hour treatment with indicated concentrations of Nutlin-3a. Bars and error bars are means and SD of N=3 independent experiments. **P<0.01; ***P<0.001, unpaired Student's *t* test between Nutlin 3a-treated *TP53*^{wt} and *TP53*$^{-/-}$ clones.

across different pediatric B-ALL subtypes, we expanded our analysis to B-ALL PDX samples, including some generated from relapsed B-ALL cases. Twelve of 14 B-ALL PDX samples exhibited sensitivity to 24-hour S3I-201 exposure (Figure 5A). Interestingly, sensitivity was apparent across a broad range of B-ALL subtypes, including *ETV6-RUNX1*$^+$ but also *TCF3-PBX1*$^+$, hyperdiploid, *KMT2A*-rearranged and *PAX5*-rearranged samples, and samples from relapsed disease. In contrast, an *ETV6-RUNX1*$^+$ and a hypodiploid B-ALL PDX sample, both from relapsed disease, exhibited resistance to STAT3 inhibition (Figure 5A). Upregulation of *CDKN1A* and *GADD45A* gene expression after 6-hour S3I-201 treatment followed the same pattern of response, changes in expression being detected in sensitive but not resistant samples (Figure 5B). Total p53 protein levels increased in all B-ALL PDX samples 6 hours after exposure to S3I-201 (*Online Supplementary Figure S6A-C*). The pattern in loss of viability was the same upon exposure of the PDX samples to Nutlin-3a, with the two S3I-201-resistant samples also exhibiting resistance to MDM2 inhibition (p53 induction) (Figure 5C). Sanger sequencing of the diagnostic relapse hypodiploid B-ALL sample from which one of the resistant PDX (sample 14) was generated, revealed the presence of a missense heterozygous *TP53* mutation (*Online Supplementary Figure S7A*). Targeted gene panel sequencing of the other resistant B-ALL PDX (sample 13), derived from relapsed *ETV6-RUNX1*$^+$ disease, detected three mutations affecting *TP53* (*Online Supplementary Figure S7B*). *TP53* missense mutations in both samples affected the region encoding the DNA-binding domain of p53, Y220C and R248Q in the hypodiploid and *ETV6-RUNX1*$^+$ samples, respectively. In contrast, targeted gene panel sequencing of the 12 sensitive PDX samples confirmed their wild-type

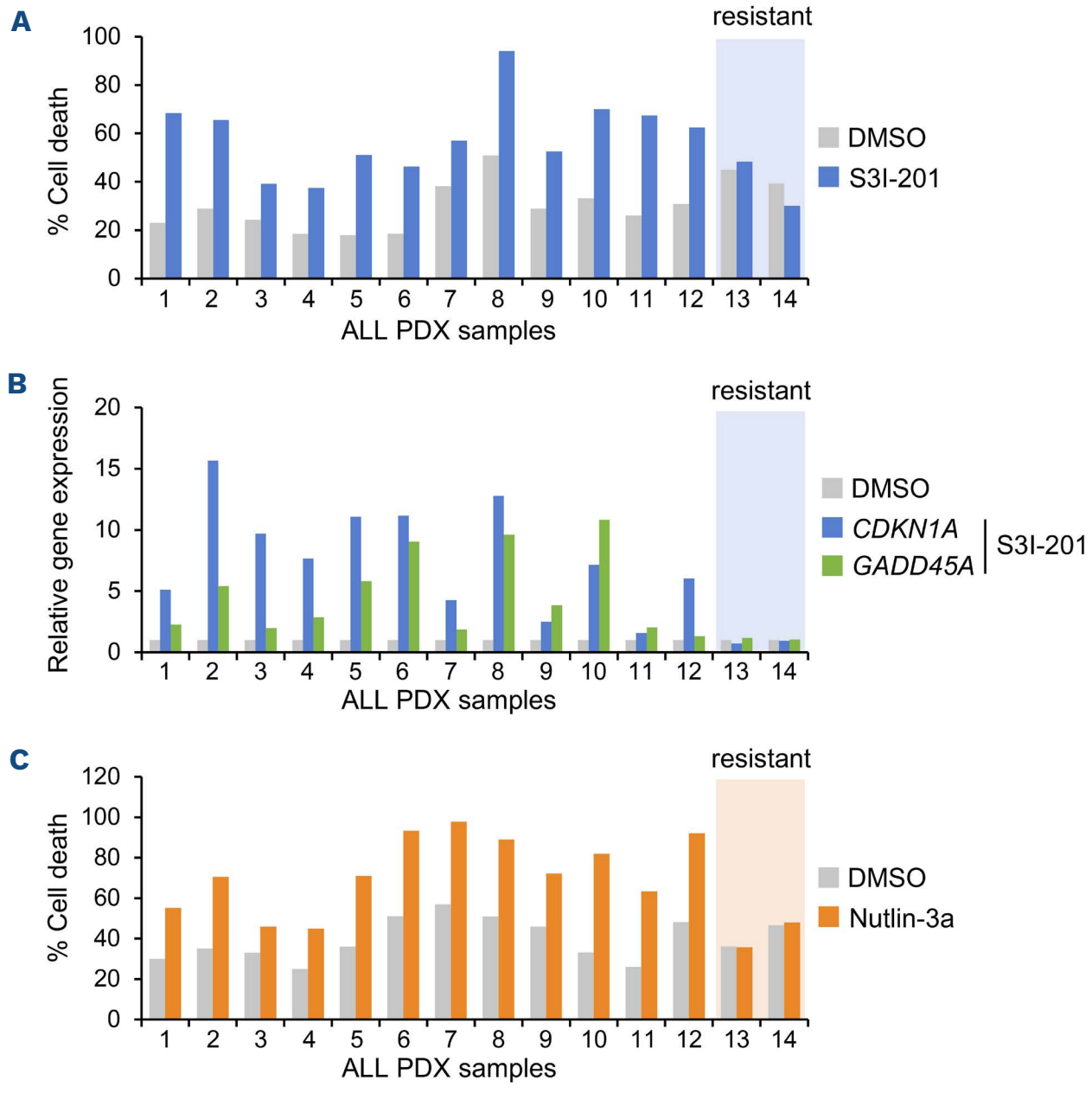

Figure 5. The sensitivity of B-cell acute lymphoblastic leukemia patient-derived xenograft cells to STAT3 inhibition correlates with *TP53* status. (A) Induction of apoptosis (% Annexin V$^+$ cells) in B-cell acute lymphoblastic leukemia patient-derived xenograft (B-ALL PDX) samples following 24-hour treatment with S3I-201 (50 μM) in liquid culture. B-ALL PDX samples: *ETV6-RUNX1*$^+$ (1-5, 12, 13), *TCF3-PBX1*$^+$ (6), hyperdiploid (7), high-hyperdiploid (8), *KMT2A-MLLT3*$^+$ (9), *KMT2A-AFDN*$^+$ (10), *PAX5*-rearranged (11) and hypodiploid (14). Samples 1-10 were derived from presentation samples and samples 11-14 from relapsed samples. (B) Quantitative real-time polymerase chain reaction (qRT-PCR) analysis of *CDKN1A* and *GADD45A* gene expression in B-ALL PDX samples following 6-hour treatment with S3I-201 (50 μM). Gene expression data are normalized to dimethyl sulfoxide (DMSO)-treated cells. (C) Induction of apoptosis (% Annexin V$^+$ cells) in B-ALL PDX samples following 24-hour treatment with Nutlin-3a (5 μM) in liquid culture.

TP53 status, although one of these (sample 11) contained a heterozygous deletion (chr17p11.2-p13.3) encompassing one *TP53* allele. Taken together, these data are consistent with a critical role of p53 in mediating B-ALL sensitivity to STAT3 inhibition.

Since p53 induction following STAT3 inhibition did not appear to be mediated via direct MDM2 modulation (*Online Supplementary Figure S4A-C*), we reasoned that it may synergize with p53 induction resulting from MDM2 inhibition. Indeed, inhibition of STAT3 by either S3I-201 or Napabucasin demonstrated synergistic anti-leukemia activity in REH cells, when combined with MDM2 inhibition by Nutlin-3a (Figure 6A, B), suggesting a rationale for combined targeting of STAT3 and MDM2 in novel B-ALL therapy.

We next used a previously developed co-culture model in which drug susceptibility of luciferase-expressing B-ALL PDX samples is evaluated after seeding onto primary Nestin-positive human MSC.[18] Five luciferase-transduced B-ALL PDX samples, two of which came from relapsed disease, proliferated over a 5-day period on human MSC (*Online Supplementary Figure S8A*). All of these samples exhibited sensitivity to C188-9[36] (also known as TTI-101), a more potent STAT3 inhibitor than S3I-201, over a similar concentration range to those reported for solid cancer cells[37] (*Online Supplementary Figure S8B*). Increased susceptibility of all five samples to STAT3 inhibition (by S3I-201, Napabucasin or C188-9) was evident on combination with MDM2 inhibition (Figure 6C). The anti-leukemia effect observed in this co-culture model was associated with cell death (*Online Supplementary Figure S8C*) and was not a consequence of a direct effect of the drugs on primary MSC viability (*data not shown*). In contrast, these drug combinations had virtually no effect on the luciferase-expressing *TP53* mutant hypodiploid B-ALL PDX (sample 14) (*Online Supplementary Figure S8D*). Similar responses to drug combinations occurred in three additional untransduced PDX samples (*Online Supplementary Figure S8E*). Longitudinal bioluminescence imaging demonstrated that short-term oral administration of Idasanutlin (MDM2 inhibitor) impaired disease progression *in vivo* in the *PAX5* rearranged (sample 11) relapsed (Figure 7) and the *KMT2A-MLLT3*$^{+}$ (sample 9) B-ALL model (*Online Supplementary Figure S9A, B*), and that in the former efficacy was improved by combining MDM2 with STAT3 inhibition.

Discussion

In this study we demonstrate that pediatric pre-B ALL exhibits broad sensitivity to STAT3 inhibition. Previously, we demonstrated that *ETV6-RUNX1*$^{+}$ B-ALL cell lines and primary patient samples were susceptible to inhibition of STAT3.[10,11] However, in contrast to cell lines,[10] the present study demonstrates that susceptibility of PDX samples is not restricted to specific subtypes of B-ALL but appears to be a general feature of the disease. Pharmacologic, shRNA- or CRISPR/Cas9-mediated inhibition of STAT3 resulted in p53 induction and cell death, largely abrogated by CRISPR-Cas9-mediated *TP53* knockout. Furthermore, two PDX samples exhibiting resistance to STAT3 inhibition were also resistant to MDM2 inhibition and contained missense *TP53* mutations. Taken together, these data indicate that p53 induction underlies the sensitivity of B-ALL cells to STAT3 inhibition.

Combined C188-9 and Idasanutlin treatment was more effective at impairing disease progression in comparison to Idasanutlin alone in the *PAX5* rearranged B-ALL PDX sample. These data validate the enhanced sensitivity of B-ALL PDX samples to combined STAT3 and MDM2 inhibition *in vitro*. However, enhanced drug combination efficacy was not seen *in vivo* for the *KMT2A-MLLT3*$^{+}$ sample and C188-9 alone did not affect disease progression in either sample. The difference in effectiveness of Idasanutlin and C188-9 *in vivo* is likely to be due to their relative bioavailabilities, further improvements of which will be required for translation of STAT3 inhibition as a therapy in B-ALL.

Evidence in the literature indicates that p53 may be regulated by STAT3 through a variety of different mechanisms. Transcriptional repression of *TP53* by STAT3 was demonstrated in Src transformed fibroblasts and melanoma cells,[23] and in chronic lymphocytic leukemia B cells.[38] More recently, leukemia inhibitory factor (LIF) was also shown to cause STAT3-dependent reduction in p53 protein expression levels in colorectal cancer cells.[39] However, in this case STAT3 activation had no effect on *TP53* mRNA levels but was rather shown to act via indirect transcriptional activation of *MDM2* and consequent p53 protein degradation.[39] Similarly, we did not observe any change in *TP53* expression in B ALL cells following STAT3 inhibition, but p53 regulation was not directly dependent on MDM2 either. However, STAT3 inhibition resulted in MDM4 protein loss that was rescued by proteasomal inhibition and was not a result of p53 induction. Since MDM4 has been shown to increase ubiquitination of p53 by MDM2, as well as directly inhibiting the transactivation activity of p53,[31] it is likely that STAT3 inhibition leads to elevated p53 protein levels by inducing MDM4 degradation. Further experiments are necessary to elucidate exactly how this is achieved.

The broad susceptibility of pediatric B-ALL PDX samples to STAT3 inhibition suggests that a requirement for STAT3 activity may be a general characteristic of the pediatric B-ALL lineage, perhaps associated with signaling pathways operating in the cells of origin. In this context it is worth noting that both STAT3 and p53 play important roles in normal B-cell development. Thus, STAT3 was shown to be involved in the positive regulation of B-cell development, deficiency resulting in a partial pre-pro-B-cell differentiation block and increased pro-B-cell apoptosis.[9] With respect to p53, regulation of its expression, transcriptionally or otherwise, plays a critical role in pre-B-cell development and selection. For example, apoptosis of pre-B cells that fail to productively rearrange their immunoglobulin heavy chain genes was shown to be mediated by p53 induction.[40] In this case, induction was via

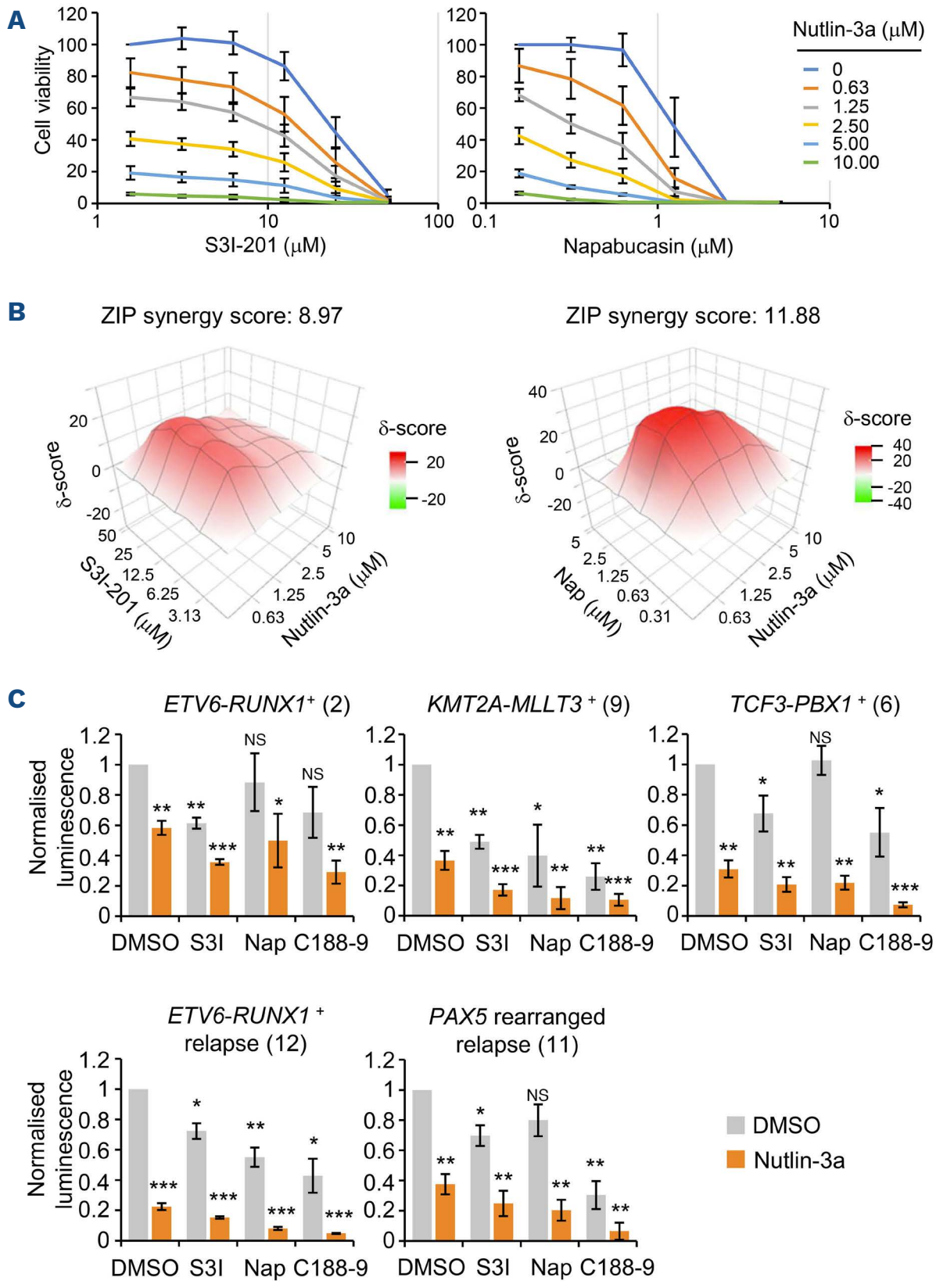

Figure 6. STAT3 and MDM2 inhibition synergize in triggering cell death in B-cell acute lymphoblastic leukemia cells. (A) Viability of REH cells following 72-hour treatment with indicated concentrations of either S3I-201 or Napabucasin in combination with Nutlin-3a. Data are normalized to dimethyl sulfoxide (DMSO)-treated cells. Graphs points and error bars are means and standard deviation (SD) of N=4 (S3I-201) and N=3 (Napabucasin) independent experiments. (B) 3D synergy maps and ZIP synergy scores of data shown in (A), calculated with SynergyFinder (version 2.0). (C) Luminescence of luciferase-expressing B-cell acute lymphoblastic leukemia patient-derived xenograft (B-ALL PDX) samples, grown in co-culture with human mesenchymal stem cells (MSC), 5 days after exposure to MDM2 inhibitor Nutlin-3a (5 μM) alone or in combination with STAT3 inhibitors S3I-201 (50 μM), Napabucasin (1.5 μM) and C188-9 (10 μM). Corresponding B-ALL PDX sample number from Figure 4 is indicated in brackets. Data are normalized to DMSO-treated cells. Bars and error bars are means and SD of N=3 independent experiments. *P<0.05; **P<0.01; ***P<0.001; NS: not significant, one sample t test.

transcriptional activation of *TP53* by the transcription factor BACH2. Furthermore, BACH2 was shown to act as a tumor suppressor in pre-B ALL, by virtue of its regulation of *TP53* expression.[40] Signaling pathways regulating p53 activity also appear to control pre-B-cell homeostasis. The Wip1 phosphatase, encoded by the p53 target gene *PPM1D*, is involved in the negative feedback regulation of p53 activation.[41] Interestingly, deletion of the *Ppm1d* gene was shown to result in reduced numbers of mature B cells. This defect was found to be due to induction of p53 and apoptosis in the pre-B-cell compartment and could be reversed by deletion of *Tp53*.[42] This suggests that the autoregulatory loop between Wip1 and

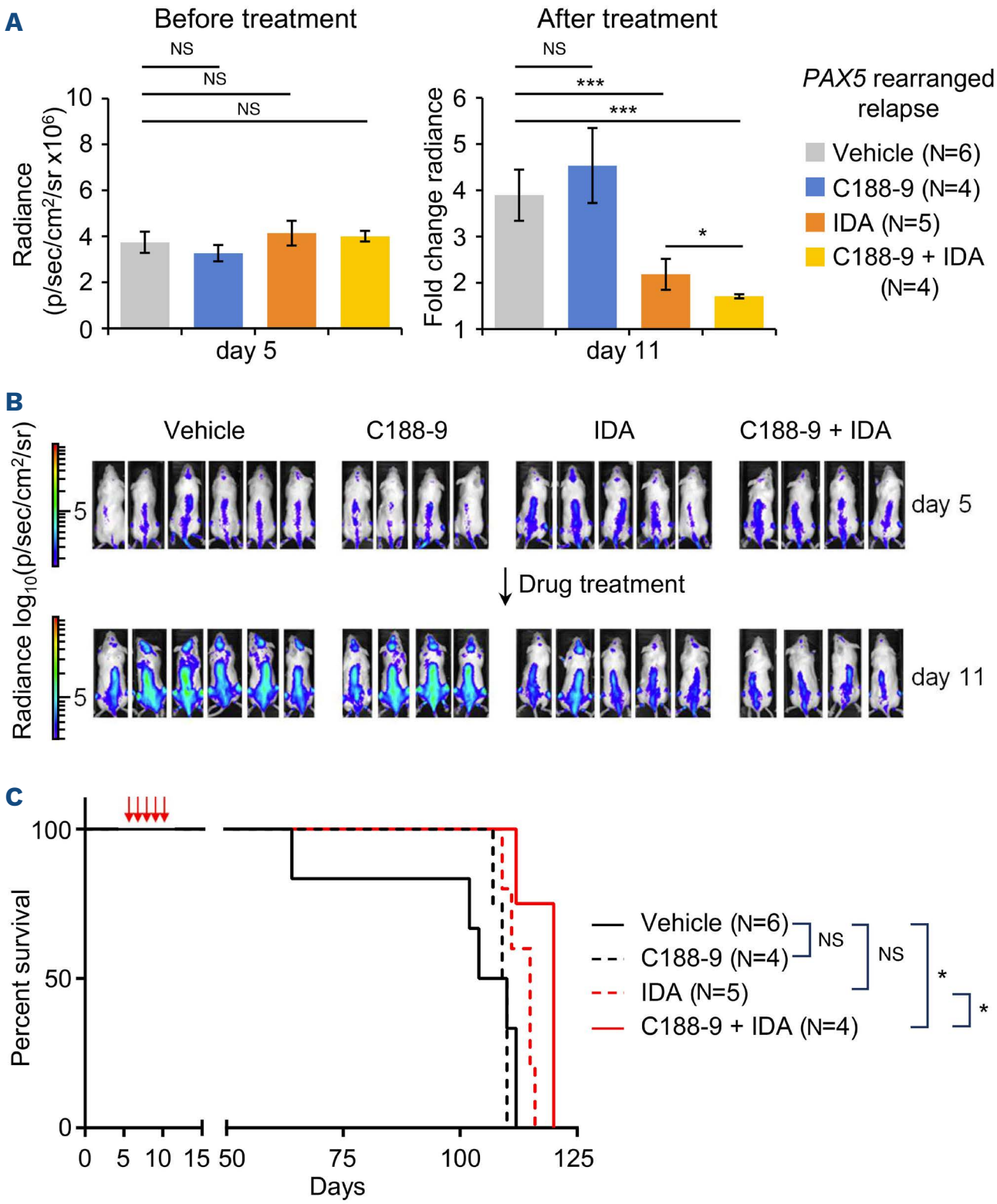

Figure 7. STAT3 and MDM2 inhibition impair B-cell acute lymphoblastic leukemia progression *in vivo*. (A) Bioluminescence signal (radiance = photons/s/cm^2/steradian) in NSG recipient mice 5 days after injection of the luciferase-expressing *PAX5* rearranged (relapse) B-cell acute lymphoblastic leukemia patient-derived xenograft (B-ALL PDX) sample and before drug treatment (left panel), and fold change in bioluminescence signal 11 days after injection, following 5 daily treatments with vehicle or the indicated drug combinations (right panel). Bars and error bars are means and standard deviation (SD) of values form each treatment group, the number of mice in each group indicated in brackets. *P< 0.05; ***P<0.001; NS: not significant, unpaired Student's t test between indicated groups. (B) Bioluminescence imaging of NSG recipient mice before (day 5) and after (day 11) drug treatment. Bars for luminescence signal represent photons/s/cm^2/steradian. (C) Survival curve for recipient mice in (A, B), treated with vehicle (black solid line), C188-9 (black dashed line), Idasanutlin (IDA, red dashed line) or C188-9 + IDA combination (red solid line). Red arrows indicate drug treatments. P=0.76 (vehicle *vs.* C188-9); P=0.055 (vehicle *vs.* IDA); P=0.0131 (vehicle *vs.* C188-9 + IDA); P=0.0494 (IDA *vs.* C188-9 + IDA), log-rank test.

p53 functions to maintain normal pre-B-cell development. In contrast to the evidence for isolated STAT3 and p53 function in normal B-cell development, relatively little is known about the possible connection between STAT3 activity and repression of p53 induction in B-cell progenitors. In this context, it is interesting to note that constitutively active STAT3 was shown to promote resistance to γ irradiation-induced apoptosis in peritoneal B-1 cells.[43] Interestingly, STAT3-dependent radioresistance could also be induced in normal B-2 B cells by stimulation with cytokines in the presence of BCR cross-linking.[43] Although p53 induction by γ irradiation was not directly examined in this study, these data suggest that a link may exist between STAT3 activity and suppression of p53 responses in normal B cells. Further studies will be required

to establish whether the STAT3/p53 pathway we describe in pre-B ALL is associated with leukemogenesis or rather is retained during transformation of pre-B cells.

TP53 mutations are more prevalent in relapsed pediatric B-ALL than primary disease.[14-16] Indeed, thiopurine chemotherapy has recently been linked with the emergence of missense *TP53* mutations.[44] However, the overall incidence of these mutations is still relatively low in comparison to other cancers,[13,45] supporting the therapeutic applicability of this approach to p53 induction in primary and relapsed pediatric B-ALL.

In conclusion, we demonstrate broad susceptibility of pediatric B ALL to p53 induction following STAT3 and combined STAT3/MDM2 inhibition. p53 induction is not a result of increased *TP53* transcription and is not directly dependent on MDM2, but rather is likely to result from MDM4 degradation. Consistent with this, B-ALL cells exhibited increased sensitivity to combined STAT3 and MDM2 inhibition *in vitro* and *in vivo*, indicating a novel disease susceptibility amenable to therapeutic exploitation.

Disclosures

No conflicts of interest to disclose.

Contributions

LG, CV, AT, NC and OW performed the experiments and data analysis. JB and DE provided clinical input and patient material. MH performed panel sequencing. JHAM analysed ChIP-sequencing data. DP and OH provided primary human MSC samples and methodology for ex vivo PDX co-culture. OW and JdB provided project leadership and supervised the research. LG and OW wrote the paper. All authors read, provided critical comments and approved the manuscript.

Acknowledgments

The authors thank Ayad Eddaoudi, UCL GOS ICH Flow Cytometry Facility, for providing assistance with flow cytometry, all the staff of the UCL GOS ICH Western Laboratories for excellent animal husbandry, and Tony Brooks and Paola Niola, UCL Genomics, for RNA and ChIP sequencing, and Deborah Hughes, Gregorz Pietka, Reda Stankunaite and Paula Proszek at Royal Marsden Hospital Center for Molecular Pathology for help with TP53 sequencing.

Funding

This research was supported by Children with Cancer UK (14-169, 17-249 to LG); Action Medical Research (GN2368 to CV); the Medical Research Council (MR/S021000/1 to CV); Children's Cancer and Leukemia Group Little Princess Trust Project Grant program (CCLGA 2022 21 to CV); SPARKS and Great Ormond Street Hospital Children's Charity (V4819 to AT); Action Medical Research and Life Arc (GN2820 to Noelia Che); Alternative Hair Charitable Foundation and Great Ormond Street Hospital Children's Charity (W1073 to JdB); Great Ormond Street Hospital Children's Charity (V1305, V2617 to OW); Olivia Hodson Cancer Fund (SR16A35 to OW); the NIHR Great Ormond Street Hospital Biomedical Research Center; and an NC3Rs fellowship (NC/P002412/1 to DP).

Data-sharing statement

The authors will make their original data available to future researchers upon request directed to the corresponding author.

References

1. Karol SE, Pui CH. Personalized therapy in pediatric high-risk B-cell acute lymphoblastic leukemia. Ther Adv Hematol. 2020;11:2040620720927575.
2. Yu H, Lee H, Herrmann A, Buettner R, Jove R. Revisiting STAT3 signalling in cancer: new and unexpected biological functions. Nat Rev Cancer. 2014;14(11):736-746.
3. Zhu F, Wang KB, Rui L. STAT3 Activation and oncogenesis in lymphoma. Cancers (Basel). 2019;12(1):19.
4. Bar-Natan M, Nelson EA, Xiang M, Frank DA. STAT signaling in the pathogenesis and treatment of myeloid malignancies. JAKSTAT. 2012;1(2):55-64.
5. Oh IH, Eaves CJ. Overexpression of a dominant negative form of STAT3 selectively impairs hematopoietic stem cell activity. Oncogene. 2002;21(31):4778-4787.
6. Chung YJ, Park BB, Kang YJ, Kim TM, Eaves CJ, Oh IH. Unique effects of Stat3 on the early phase of hematopoietic stem cell regeneration. Blood. 2006;108(4):1208-1215.
7. Kortylewski M, Kujawski M, Wang T, et al. Inhibiting Stat3 signaling in the hematopoietic system elicits multicomponent antitumor immunity. Nat Med. 2005;11(12):1314-1321.
8. Frank DA. STAT3 as a central mediator of neoplastic cellular transformation. Cancer Lett. 2007;251(2):199-210.
9. Chou WC, Levy DE, Lee CK. STAT3 positively regulates an early step in B-cell development. Blood. 2006;108(9):3005-3011.
10. Mangolini M, de Boer J, Walf-Vorderwulbecke V, Pieters R, den Boer ML, Williams O. STAT3 mediates oncogenic addiction to TEL-AML1 in t(12;21) acute lymphoblastic leukemia. Blood. 2013;122(4):542-549.
11. Virely C, Gasparoli L, Mangolini M, et al. ARHGEF4 regulates an essential oncogenic program in t(12;21)-associated acute lymphoblastic leukemia. Hemasphere. 2020;4(5):e467.
12. Bhansali RS, Rammohan M, Lee P, et al. DYRK1A regulates B cell acute lymphoblastic leukemia through phosphorylation of FOXO1 and STAT3. J Clin Invest. 2021;131(1):e135937.
13. Imamura J, Miyoshi I, Koeffler HP. p53 in hematologic malignancies. Blood. 1994;84(8):2412-2421.
14. Gump J, McGavran L, Wei Q, Hunger SP. Analysis of TP53 mutations in relapsed childhood acute lymphoblastic leukemia. J Pediatr Hematol Oncol. 2001;23(7):416-419.
15. Hof J, Krentz S, van Schewick C, et al. Mutations and deletions of the TP53 gene predict nonresponse to treatment and poor outcome in first relapse of childhood acute lymphoblastic leukemia. J Clin Oncol. 2011;29(23):3185-3193.
16. Krentz S, Hof J, Mendioroz A, et al. Prognostic value of genetic

alterations in children with first bone marrow relapse of childhood B-cell precursor acute lymphoblastic leukemia. Leukemia. 2013;27(2):295-304.
17. Bomken S, Buechler L, Rehe K, et al. Lentiviral marking of patient-derived acute lymphoblastic leukaemic cells allows in vivo tracking of disease progression. Leukemia. 2013;27(3):718-721.
18. Pal D, Blair HJ, Elder A, et al. Long-term in vitro maintenance of clonal abundance and leukaemia-initiating potential in acute lymphoblastic leukaemia. Leukemia. 2016;30(8):1691-1700.
19. Walf-Vorderwulbecke V, Pearce K, Brooks T, et al. Targeting acute myeloid leukemia by drug-induced c-MYB degradation. Leukemia. 2018;32(4):882-889.
20. Clesham K, Walf-Vorderwulbecke V, Gasparoli L, et al. Identification of a c-MYB-directed therapeutic for acute myeloid leukemia. Leukemia. 2022;36(6):1541-1549.
21. Siddiquee K, Zhang S, Guida WC, et al. Selective chemical probe inhibitor of Stat3, identified through structure-based virtual screening, induces antitumor activity. Proc Natl Acad Sci U S A. 2007;104(18):7391-7396.
22. Fischer M. Census and evaluation of p53 target genes. Oncogene. 2017;36(28):3943-3956.
23. Niu G, Wright KL, Ma Y, et al. Role of Stat3 in regulating p53 expression and function. Mol Cell Biol. 2005;25(17):7432-7440.
24. Li Y, Rogoff HA, Keates S, et al. Suppression of cancer relapse and metastasis by inhibiting cancer stemness. Proc Natl Acad Sci U S A. 2015;112(6):1839-1844.
25. Haupt Y, Maya R, Kazaz A, Oren M. Mdm2 promotes the rapid degradation of p53. Nature. 1997;387(6630):296-299.
26. Kubbutat MH, Jones SN, Vousden KH. Regulation of p53 stability by Mdm2. Nature. 1997;387(6630):299-303.
27. Honda R, Tanaka H, Yasuda H. Oncoprotein MDM2 is a ubiquitin ligase E3 for tumor suppressor p53. FEBS Lett. 1997;420(1):25-27.
28. Lane DP, Hall PA. MDM2--arbiter of p53's destruction. Trends Biochem Sci. 1997;22(10):372-374.
29. Barak Y, Juven T, Haffner R, Oren M. mdm2 expression is induced by wild type p53 activity. EMBO J. 1993;12(2):461-468.
30. Wu X, Bayle JH, Olson D, Levine AJ. The p53-mdm-2 autoregulatory feedback loop. Genes Dev. 1993;7(7A):1126-1132.
31. Haupt S, Mejia-Hernandez JO, Vijayakumaran R, Keam SP, Haupt Y. The long and the short of it: the MDM4 tail so far. J Mol Cell Biol. 2019;11(3):231-244.
32. Chuikov S, Kurash JK, Wilson JR, et al. Regulation of p53 activity through lysine methylation. Nature. 2004;432(7015):353-360.
33. el-Deiry WS, Tokino T, Velculescu VE, et al. WAF1, a potential mediator of p53 tumor suppression. Cell. 1993;75(4):817-825.
34. Nakano K, Vousden KH. PUMA, a novel proapoptotic gene, is induced by p53. Mol Cell. 2001;7(3):683-694.
35. Zhang C, Gao C, Kawauchi J, Hashimoto Y, Tsuchida N, Kitajima S. Transcriptional activation of the human stress-inducible transcriptional repressor ATF3 gene promoter by p53. Biochem Biophys Res Commun. 2002;297(5):1302-1310.
36. Redell MS, Ruiz MJ, Alonzo TA, Gerbing RB, Tweardy DJ. Stat3 signaling in acute myeloid leukemia: ligand-dependent and -independent activation and induction of apoptosis by a novel small-molecule Stat3 inhibitor. Blood. 2011;117(21):5701-5709.
37. Lewis KM, Bharadwaj U, Eckols TK, et al. Small-molecule targeting of signal transducer and activator of transcription (STAT) 3 to treat non-small cell lung cancer. Lung Cancer. 2015;90(2):182-190.
38. Sainz-Perez A, Gary-Gouy H, Gaudin F, et al. IL-24 induces apoptosis of chronic lymphocytic leukemia B cells engaged into the cell cycle through dephosphorylation of STAT3 and stabilization of p53 expression. J Immunol. 2008;181(9):6051-6060.
39. Yu H, Yue X, Zhao Y, et al. LIF negatively regulates tumour-suppressor p53 through Stat3/ID1/MDM2 in colorectal cancers. Nat Commun. 2014;5:5218.
40. Swaminathan S, Huang C, Geng H, et al. BACH2 mediates negative selection and p53-dependent tumor suppression at the pre-B cell receptor checkpoint. Nat Med. 2013;19(8):1014-1022.
41. Takekawa M, Adachi M, Nakahata A, et al. p53-inducible wip1 phosphatase mediates a negative feedback regulation of p38 MAPK-p53 signaling in response to UV radiation. EMBO J. 2000;19(23):6517-6526.
42. Yi W, Hu X, Chen Z, et al. Phosphatase Wip1 controls antigen-independent B-cell development in a p53-dependent manner. Blood. 2015;126(5):620-628.
43. Otero DC, Poli V, David M, Rickert RC. Cutting edge: inherent and acquired resistance to radiation-induced apoptosis in B cells: a pivotal role for STAT3. J Immunol. 2006;177(10):6593-6597.
44. Yang F, Brady SW, Tang C, et al. Chemotherapy and mismatch repair deficiency cooperate to fuel TP53 mutagenesis and ALL relapse. Nat Cancer. 2021;2(8):819-834.
45. Comeaux EQ, Mullighan CG. TP53 Mutations in hypodiploid acute lymphoblastic leukemia. Cold Spring Harb Perspect Med. 2017;7(3):a026286.